AIAA JOURNAL
Vol. 36, No. 6, June 1998

Helicopter Rotor System Fault Detection Using Physics-Based Model and Neural Networks

Ranjan Ganguli* and Inderjit Chopra†
University of Maryland, College Park, Maryland 20742
and
David J. Haas‡
U.S. Naval Surface Warfare Center, Bethesda, Maryland 20084

A comprehensive physics-based model of the helicopter rotor in forward flight is used to analyze the impact of selected faults on rotor system behavior. The rotor model is based on finite elements in space and time. The helicopter rotor model is used to develop a neural network-based damage detection methodology. Simulated data from the rotor system are contaminated with noise and used to train a feedforward neural network using backpropogation learning. Cases considered for training and testing the neural network include both single and multiple faults on the damaged blade. Results show that the neural network can detect and quantify both single and multiple faults on the blade from noise-contaminated simulated vibration and blade response test data. For accurate estimation of type and extent of damages, it is important to train the neural networks with noise-contaminated response data.

Nomenclature

C_T = thrust coefficient
d = damage level
e = error
e_{id} = error in damage identification
F = hub forces
F_x = longitudinal hub force
F_y = lateral hub force
F_z = vertical hub force
M = hub moments
M_x = rolling hub moment
M_y = pitching hub moment
M_z = yawing hub moment
m = number of damage types
N = number of spatial finite elements, number of damage levels for training data
N_b = number of blades
N_e = number of errors in damage detection
$\mathcal{N}$ = neural network mapping
$\boldsymbol{P}$ = input matrix for neural network
$\boldsymbol{p}$ = system response vector
R = rotor radius
T = kinetic energy, target matrix for neural network
U = strain energy
v = lag deformation of blade
W = virtual work
w = flap deformation of blade
x = blade spanwise coordinate
α = angle of attack, noise level
Δ = difference between damaged and undamaged quantity
δ = variation
μ = advance ratio
σ = solidity ratio
ϕ = torsional deformation of blade, activation function
ψ = azimuth angle, time
Ω = rotation speed
$\angle$ = change in phase angle

Subscripts

ic = ith cosine component
is = ith sine component
n = noise contaminated quantity
test = related to test data
tr = related to training data
0 = zeroth harmonic, steady quantity

Introduction

HELICOPTER rotors are subject to high vibratory forces because of highly flexible rotating blades and a severe aerodynamic environment. This leads to wear in various components of the rotor, requiring frequent inspection and replacement of damage sensitive components leading to high-maintenance costs. In fact, maintenance costs account for about one-quarter of the direct operating costs of rotorcraft.[1,2] Health and usage monitoring systems (HUMS) can reduce this cost. The helicopter industry has recently focused on HUMS to provide fault diagnosis for drivetrain, engines, oil system, and rotor system.[3,4] Current track and balance systems can detect rotor faults to a limited extent. For example, when track and balance adjustments do not alleviate a high-vibration problem, a faulty component may be indicated. To develop a health monitoring system for a rotor, the relationship between blade damage and helicopter system behavior is needed. Because it is difficult to obtain flight-test data for a damaged helicopter rotor, a physics-based model offers the opportunity to study the simulated behavior of the damaged helicopter. Numerical simulations of the damaged rotor system response can be used by artificial-intelligence-based techniques such as neural networks to learn the relationship between rotor faults and system behavior. The trained neural network can then be placed online on the helicopter to detect and identify damage from rotor vibration and response data.

The fault detection methodology approach just discussed focuses on global faults. Global faults are those that can be detected using remote measurements of global system parameters such as fuselage vibration and blade deflection. The theoretical basis of global fault detection is that for an undamaged rotor all blades will have identical response and only the N/revolution loads will be transmitted to the hub by an N-bladed rotor. If, however, one blade is dissimilar to the other blades due to a fault, then all harmonics of the rotor loads are transmitted to the hub. In addition, the response of the damaged blade will be different from the undamaged blades.

Received Sept. 27, 1996; revision received Feb. 15, 1998; accepted for publication Feb. 17, 1998.

*Assistant Research Scientist, Alfred Gessow Rotorcraft Center, Department of Aerospace Engineering; currently Mechanical Engineer, General Electric Corporate R&D Center, Niskayuna, NY 12309. Member AIAA.

†Professor and Director, Alfred Gessow Rotorcraft Center, Department of Aerospace Engineering. Fellow AIAA.

‡Aerospace Engineer, Sea Based Aviation Office, Carderock Division. Senior Member AIAA.

Selected works on global fault simulation have been reported in the literature.[5–7] Azzam and Andrew[5] simulated rotor system faults for a five-bladed articulated rotor similar to the S-61 rotor using a computer-based mathematic–dynamic model. Faults modeled include blade cracks, chordwise mass imbalance, and defective lag damper. The present authors have applied a comprehensive aeroelastic analysis based on finite element in space and time to simulate a damaged rotor.[6,7] Numerical results were obtained in hover and in forward flight for an articulated four-bladed rotor similar to the SH-60 rotor. Selected predictions of rotor component loads were validated with flight-test data.[6] Faults modeled in Ref. 6 include moisture absorption, loss of trim mass, damaged pitch-control system, defective lag damper, damaged trim tab, and misadjusted pitch link. Faults modeled in Ref. 7 include aerodynamic mistracking, blade crack, stiffness defect, manufacturing defect, and chordwise mass imbalance. The influence of simulated rotor faults on blade response and vibratory hub loads was analyzed and summarized in the form of diagnostic charts. It was concluded that most rotor faults can be detected by monitoring blade response and vibration. However, localized damage such as blade cracks are difficult to detect from global system behavior.

The cited studies focused on calculation of rotor response due to simulated rotor system faults. However, there is a need to use the simulated data to develop a fault detection methodology. Addressing this issue, the present authors developed a neural network-based approach for rotor system fault detection.[8] Two neural networks were used, the first network to classify the type of fault and the second network to characterize the level of damage. The neural networks are trained from a numerically generated rotor system fault database. One drawback of a neural network trained with ideal data is that it classifies ideal test data exactly, but gives significant errors when noise is added to the test data. This problem was overcome by adding noise to the analytical simulation during training. A fault detection system based on noisy simulated data was found to be more robust than that developed using ideal simulated data because it accounts for the inherent uncertainty in the real system. Testing of the trained neural network showed that it can detect and identify damage in the rotor system from simulated blade response and vibration data.

In addition to global faults such as those discussed, there are local faults, which are difficult to detect from global system behavior such as fuselage vibration and rotor response.[9] Localized structural damage such as blade cracks and delamination are examples of local faults. Undetected blade cracks can lead to catastrophic failure depending on crack location, flight conditions, and load severity. Local fault detection methods have evolved to detect such faults. The methods used for local fault detection include robust laser interferometer, photoelastic techniques, ultrasonic techniques, and acoustic emission sensors.[10] Such local fault detection techniques complement the global fault detection approach discussed in this paper. When combined together, they can form a comprehensive approach to rotor system health monitoring.

The damage detection techniques discussed in previous research focused on primary faults (only one type of fault on the blade).[8] In this paper, the detection of compound faults is addressed. Compound faults involve more that one type of fault on the damaged blade. Detecting the components with a compound fault is important for distinguishing between benign faults (such as track and balance problems) and potentially catastrophic faults (such as damaged lag damper).

Formulation

Mathematical Model of Rotor System

The helicopter is represented by a nonlinear model of several elastic rotor blades dynamically coupled to a six-degree-of-freedom rigid fuselage. Each blade undergoes flap bending, lag bending, elastic twist, and axial displacement. Formulation is based on a generalized Hamilton's principle applicable to nonconservative systems,

$$\int_{\psi_1}^{\psi_2} (\delta U - \delta T - \delta W)\, \mathrm{d}\psi = 0 \tag{1}$$

where δU, δT, and δW are virtual strain energy, kinetic energy, and virtual work, respectively. Here δU and δT also include energy contributions from components that are attached to the blade, e.g., pitch link, lag damper, etc. External aerodynamic forces on the rotor blade contribute to the virtual work variational δW. For the aeroelastic analysis, aerodynamic forces and moments are calculated using an inflow distribution from the Scully–Johnson free-wake model[11] and unsteady effects are accounted for using the Leishman–Beddoes[12] model.

Finite element methodology is used to discretize the governing equations of motion and allows for accurate representation of complex hub kinematics and nonuniform blade properties. After finite element discretization, Hamilton's principle is written as

$$\int_{\psi_i}^{\psi_f} \sum_{i=1}^{N} (\delta U_i - \delta T_i - \delta W_i)\, \mathrm{d}\psi = 0 \tag{2}$$

Each beam element has 15 degrees of freedom. These degrees of freedom correspond to cubic variations in axial elastic and (flap and lag) bending deflections and quadratic variation in elastic torsion.

The first step in the aeroelastic analysis procedure is to trim the vehicle for the specified operating condition. The blade finite element equations are transformed to normal mode space for efficient solution of the blade response. The nonlinear, periodic, normal mode equations are then solved for steady response using a finite element in time method. Steady and vibratory components of the rotating frame blade loads, i.e., shear forces and bending/torsion moments, are calculated using the force summation method. In this approach, blade aerodynamic and inertia forces are integrated directly over the length of the blade. Fixed frame hub loads are calculated by summing the contributions of individual blades. A coupled trim procedure is carried out to solve simultaneously for the blade response, pilot input trim controls, and vehicle orientation. The coupled trim procedure is essential for elastically coupled blades because elastic deflections play an important role in the steady net forces and moments generated by the rotor.

Indicators of System Damage

It is assumed that one blade is damaged and the other blades are undamaged. For the undamaged rotor (assuming perfectly tracked blades), all four blades will have identical tip response (magnitude and phase). Also, for a perfectly tracked rotor, only 4/revolution and 8/revolution forces and moments will be transmitted by the undamaged rotor to the fuselage.

In practice, however, there will always be some level of fuselage response at 1/revolution and at higher harmonics due to the inability to perfectly balance and track a rotor. Typically, a 1/revolution fuselage response of 0.15 ips, equivalent to about 170 lb, is representative of a well-balanced rotor. Vibrations in excess of 0.30 ips are considered significant and indicate the need to track and balance the rotor. Approximate thresholds for the moments transmitted to the fuselage can be similarly obtained. Moments below 2500 lb-in. are representative of a well-tracked and balanced rotor. Moments above 5000 lb-in. indicate the need to track and balance the rotor.

Similarly, for the blade tip response, most real rotors display some degree of variation in tip displacements between blades even when the rotor is considered to be in a tracked condition. In this study, we assume that variations in tip deflections less than one-quarter of an inch are negligible, and changes in elastic twist of less than one-quarter of a degree are considered too small to be of practical value. These measures for system response are shown in Table 1.

The vibratory hub loads and blade response predicted by the mathematical model are assembled into the following vector form:

$$\boldsymbol{p} = \lfloor \Delta v\, \Delta w\, \Delta\phi\, F_x\, F_y\, F_z\, M_x\, M_y\, M_z \rfloor^T \tag{3}$$

Blade response harmonics greater than 5 and load harmonics greater than 10 are very small and are neglected. The change in blade tip response between the damaged and undamaged blade is expressed in the form (for flap response)

$$\Delta w = \lfloor \Delta w_0\, \Delta w_{1c}\, \Delta w_{1s}\, \Delta w_{2c}\, \Delta w_{2s}\, \Delta w_{3c}\, \Delta w_{3s} \times \Delta w_{4c}\, \Delta w_{4s}\, \Delta w_{5c}\, \Delta w_{5s} \rfloor^T \tag{4}$$

Table 1 Quantitative measures for system behavior

Measure (units)	Tip flap, lag, in.	Tip torsion, deg	Forces, lb	Moments, lb-in.	Phase, deg	Symbols
Negligible	<0.25	<0.25	<170	<2500	<10	~
Moderate	0.25–0.50	0.25–0.50	170–340	2500–5000	10–30	○
Significant	>0.50	>0.50	>340	>5000	>30	◯

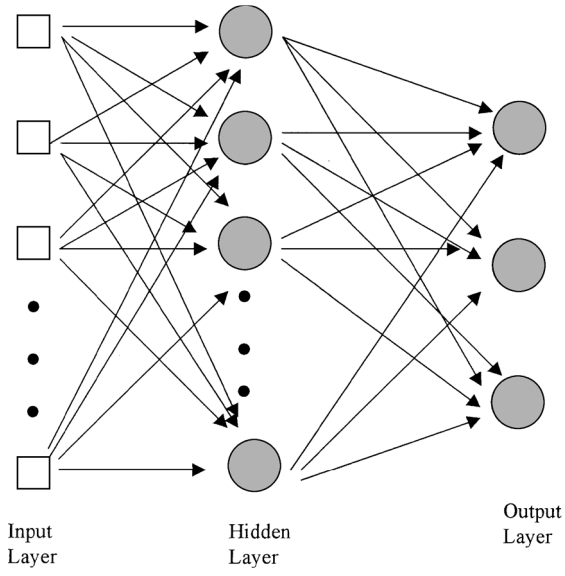

Fig. 1 Schematic representation of multilayer neural network.

The blade lag and torsion response can be similarly expressed. The vector for the longitudinal force is given as

$$\boldsymbol{F}_x = \lfloor F_{x0} F_{x1c} F_{x1s} F_{x2c} F_{x2s} F_{x3c} F_{x3s} F_{x4c} F_{x4s} F_{x5c} F_{x5s} F_{x6c} F_{x6s} \times F_{x7c} F_{x7s} F_{x8c} F_{x8s} F_{x9c} F_{x9s} F_{x10c} F_{x10s} \rfloor^T \quad (5)$$

Similar vectors define the other forces and moments. The vector $\boldsymbol{p}$ in Eq. (3) has 159 elements and contains the needed information about the damaged rotor system in mathematical form.

To simulate data contaminated by noise, zero-mean white noise with a normal distribution is added to $\boldsymbol{p}$. The noise is added to each element of the $\boldsymbol{p}$ vector as follows:

$$\boldsymbol{p}_{ni} = \boldsymbol{p}_i + \boldsymbol{p}_i \alpha \epsilon = \boldsymbol{p}_i (1 + \alpha \epsilon) \quad (6)$$

where ϵ is a random number between -1 and 1 from the normal distribution and α is the noise level. A value of α of 0.05 is referred to as 5% noise and implies an uncertainty of 5% in the data for $\boldsymbol{p}_i$. The noisy response vector is denoted by $\boldsymbol{p}_n$.

Neural Network Architecture

Two neural networks are used for the damage detection problem. Both networks consists of an input layer, a hidden layer, and an output layer. A schematic of the network is shown in Fig. 1. The first network (network A) is a pattern classifier. Network A determines the type (or types) of damage, for example, whether the damage is moisture absorption or a defective lag damper, or a combination of both. For network A, the hidden layer and the output layer consist of nonlinear logarithmic sigmoid neurons, an architecture known to be suitable for pattern classification.[13] These neurons use sigmoid activation functions of the type

$$\phi(v) = \frac{1}{1 + \exp(-v)} \quad (7)$$

The second network (network B) is a function approximator. For network B, the hidden layer consists of nonlinear log-sigmoid neurons and the output layer consists of linear neurons, an architecture known to be suitable for function approximation problems. Network B assumes that network A has isolated the type of damage and uses this information to determine the magnitude of damage. This procedure is shown schematically in Fig. 2.

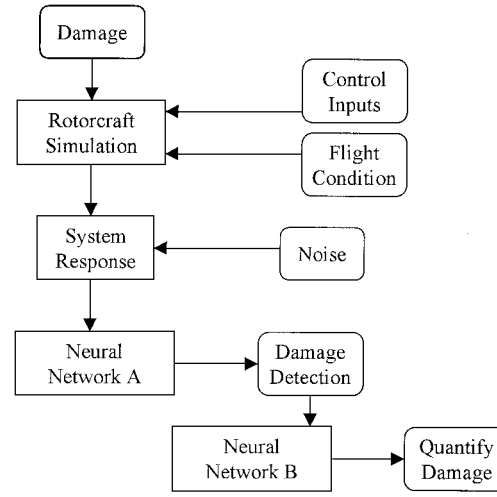

Fig. 2 Schematic representation of model-based damage detection procedure.

A backpropagation algorithm with added momentum and an adaptive learning rate is used.[14] The error measure of the networks is defined as

$$e_k = \frac{\|\boldsymbol{t} - \boldsymbol{t}'_k\|}{\|\boldsymbol{t}\|} \quad (8)$$

where $\boldsymbol{t}$ is the desired target vector and $\boldsymbol{t}'_k$ is the output vector produced by the network at the end of the kth iteration and where $\|\cdot\|$ is the Euclidean norm. The algorithm is assumed to have converged when the error becomes sufficiently small ($e_k = 0.00001$).

Training Database

Three representative rotor faults are used to train the neural network: moisture absorption, defective lag damper, and damaged pitch-control system. In each case, training data are generated by starting with an undamaged rotor and progressively increasing the damage intensity on the damaged blade.

The training target vectors are defined as

$$\boldsymbol{d} = \lfloor 0 \quad 0.1 \quad 0.2 \quad \cdots \quad 0.9 \quad 1.0 \rfloor \quad (9)$$

The value 0 corresponds to the undamaged case and 1.0 corresponds to significant damage. Intermediate values of $\boldsymbol{d}$ represents a linear variation in the damage magnitude between these extremes. For moisture absorption, $\boldsymbol{d}_i = 1$ corresponds to an increase in mass of the damaged blade by 3%, compared to the undamaged blade. For the defective lag damper, $\boldsymbol{d}_i = 0$ corresponds to a lag damping constant $C_\zeta = 3000$ lb s/in., and $\boldsymbol{d}_i = 1$ corresponds to a lag damper constant C_ζ of the damaged blade equal to zero. For the pitch-control system, damage level is represented by a linear reduction in pitch-link stiffness from 100% for the undamaged blade to 12% for the damaged blade. This corresponds to a reduction in the baseline torsion frequency from 4.31 per revolution for the undamaged blade ($\boldsymbol{d}_i = 0$) to 4.0 per revolution for the damaged blade ($\boldsymbol{d}_i = 1$). The variation of the first torsion mode frequency with pitch-control system damage level is shown in Fig. 3. The aeroelastic analysis is performed for the values of $\boldsymbol{d}$ defined earlier and for each case the system response vector $\boldsymbol{p}$ defined by Eq. (3) is calculated. These data form the simulated fault database. The database is divided into

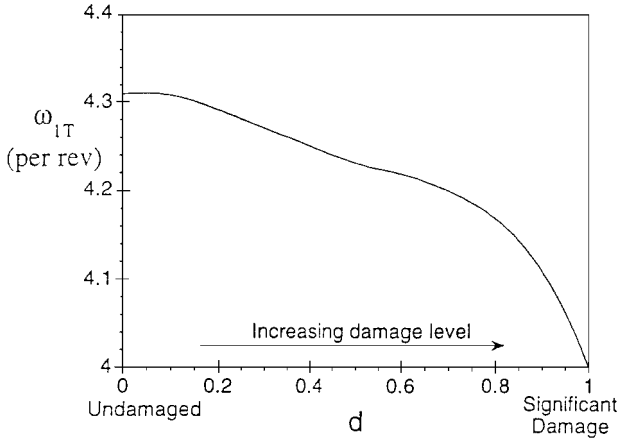

Fig. 3 First rotating torsion frequency of blade with damaged pitch-control system.

two parts depending on the value of $\boldsymbol{d}$. One part is used for training the neural network [Eq. (10)] and the other for testing the trained neural network [Eq. (11)]:

$$\boldsymbol{d}_{\text{tr}} = \lfloor 0 \quad 0.2 \quad 0.4 \quad 0.6 \quad 0.8 \quad 1.0 \rfloor \tag{10}$$

$$\boldsymbol{d}_{\text{test}} = \lfloor 0.1 \quad 0.3 \quad 0.5 \quad 0.7 \quad 0.9 \rfloor \tag{11}$$

For each damage type, six damage levels are used for training and five damage levels are used for testing. When there is more than a single fault on the damaged blade, the data needed for training the neural network become large as the number of faults increases. For example, for two faults on the damaged blade, there are 36 (6×6) combinations of damage levels for training and 25 (5×5) for testing the neural network.

Damage Detection

Neural network A is used for damage detection. The input to the neural network is the vector $\boldsymbol{p}$, defined at N damage levels [Eq. (10)], for the three damages being considered. The input matrix $\boldsymbol{P}$ is given as

$$\boldsymbol{P} = [\boldsymbol{P}_1 \quad \boldsymbol{P}_2 \quad \boldsymbol{P}_3 \quad \boldsymbol{P}_{12} \quad \boldsymbol{P}_{13} \quad \boldsymbol{P}_{23}] \tag{12}$$

where for damage 1

$$\boldsymbol{P}_1 = [\boldsymbol{p}_1 \quad \boldsymbol{p}_2 \quad \cdots \quad \boldsymbol{p}_N]$$

for damage 2

$$\boldsymbol{P}_2 = [\boldsymbol{p}_1 \quad \boldsymbol{p}_2 \quad \cdots \quad \boldsymbol{p}_N]$$

and for damage 3

$$\boldsymbol{P}_3 = [\boldsymbol{p}_1 \quad \boldsymbol{p}_2 \quad \cdots \quad \boldsymbol{p}_N]$$

Each matrix $\boldsymbol{P}_k$ shown has 159 rows and N columns and represents a single fault on the damaged blade. For the case with two faults on the damaged blade, the input matrices for damages 1 and 2 are

$$\boldsymbol{P}_{12} = \begin{bmatrix} \boldsymbol{p}_{11} & \boldsymbol{p}_{12} & \cdots & \boldsymbol{p}_{1N} \\ \boldsymbol{p}_{21} & \boldsymbol{p}_{22} & \cdots & \boldsymbol{p}_{2N} \\ \vdots & \vdots & \vdots & \vdots \\ \boldsymbol{p}_{N1} & \boldsymbol{p}_{N2} & \cdots & \boldsymbol{p}_{NN} \end{bmatrix} \tag{13}$$

for damages 1 and 3 are

$$\boldsymbol{P}_{13} = \begin{bmatrix} \boldsymbol{p}_{11} & \boldsymbol{p}_{12} & \cdots & \boldsymbol{p}_{1N} \\ \boldsymbol{p}_{21} & \boldsymbol{p}_{22} & \cdots & \boldsymbol{p}_{2N} \\ \vdots & \vdots & \vdots & \vdots \\ \boldsymbol{p}_{N1} & \boldsymbol{p}_{N2} & \cdots & \boldsymbol{p}_{NN} \end{bmatrix} \tag{14}$$

and for damages 2 and 3 are

$$\boldsymbol{P}_{23} = \begin{bmatrix} \boldsymbol{p}_{11} & \boldsymbol{p}_{12} & \cdots & \boldsymbol{p}_{1N} \\ \boldsymbol{p}_{21} & \boldsymbol{p}_{22} & \cdots & \boldsymbol{p}_{2N} \\ \vdots & \vdots & \vdots & \vdots \\ \boldsymbol{p}_{N1} & \boldsymbol{p}_{N2} & \cdots & \boldsymbol{p}_{NN} \end{bmatrix} \tag{15}$$

Each matrix $\boldsymbol{P}_{ij}$ has 159 rows and $N \times N$ columns. The element $\boldsymbol{p}_{ij}$ represents the system response vector $\boldsymbol{p}$ for two damages at damage levels i and j. In each case, i and j range from 1 to N. The target vector $\boldsymbol{T}$ is given as

$$\boldsymbol{T} = \begin{bmatrix} \lfloor \mathbf{1} \rfloor & \lfloor \mathbf{0} \rfloor & \lfloor \mathbf{0} \rfloor & \lfloor \mathbf{1} \rfloor & \lfloor \mathbf{1} \rfloor & \lfloor \mathbf{0} \rfloor \\ \lfloor \mathbf{0} \rfloor & \lfloor \mathbf{1} \rfloor & \lfloor \mathbf{0} \rfloor & \lfloor \mathbf{1} \rfloor & \lfloor \mathbf{0} \rfloor & \lfloor \mathbf{1} \rfloor \\ \lfloor \mathbf{0} \rfloor & \lfloor \mathbf{0} \rfloor & \lfloor \mathbf{1} \rfloor & \lfloor \mathbf{0} \rfloor & \lfloor \mathbf{1} \rfloor & \lfloor \mathbf{1} \rfloor \end{bmatrix} \tag{16}$$

where

$$\lfloor \mathbf{1} \rfloor = \{1 \quad 1 \quad \cdots \quad 1\} \tag{17}$$

$$\lfloor \mathbf{0} \rfloor = \{0 \quad 0 \quad \cdots \quad 0\} \tag{18}$$

Here $\lfloor \mathbf{1} \rfloor$ and $\lfloor \mathbf{0} \rfloor$ are row vectors of size N or size $N \times N$, depending on the nature of the fault (primary or compound). The row in which $\mathbf{1}$ is present in the $\boldsymbol{T}$ matrix corresponds to the type of damage. The neural network performs a mapping of training vector $\boldsymbol{P}$ into target vector $\boldsymbol{T}$ and can be written as

$$\boldsymbol{T} = \mathcal{N}(\boldsymbol{P}) \tag{19}$$

where $\mathcal{N}$ is the neural network mapping. The effect of noise is included by defining an augmented training matrix

$$\boldsymbol{P}_n = \lfloor \boldsymbol{P} \quad \boldsymbol{P} \quad \boldsymbol{P}' \quad \boldsymbol{P}'' \rfloor \tag{20}$$

where $\boldsymbol{P}'$ and $\boldsymbol{P}''$ are noise contaminated signals defined as $(\boldsymbol{P}')_i = (\boldsymbol{P})_i + (\boldsymbol{P})_i\, 0.05\epsilon$ and where $(\boldsymbol{P}'')_i = (\boldsymbol{P})_i + (\boldsymbol{P})_i\, 0.1\epsilon$ represent 5 and 10% noise contamination, respectively. The augmented training matrix contains two copies of the ideal matrix and two noisy matrices. These inputs are all matched to the same target outputs. The augmented target vector is obtained as

$$\boldsymbol{T}_n = \lfloor \boldsymbol{T} \quad \boldsymbol{T} \quad \boldsymbol{T} \quad \boldsymbol{T} \rfloor \tag{21}$$

The network mapping with noisy data can now be represented as

$$\boldsymbol{T}_n = \mathcal{N}_n(\boldsymbol{P}_n) \tag{22}$$

For each fault, the pattern from only ideal data is expanded by adding noise contaminated data. The neural network is trained to map these patterns with the faults causing them. For training the network, the following procedure is followed. First, the network is trained using ideal data, as shown in Eq. (19). Next, the network is trained on noisy data for 10 cycles, as shown in Eq. (22). For each training cycle, the converged weights are used as the starting values from the previous cycle. For each cycle, a different randomly generated seed value is used by the random number generator to form the noisy data. The 10 cycles provide considerable noisy training data and generalize the input patterns mapping onto the faults. Finally, to ensure that the network recognizes the ideal vectors, it is again trained on ideal data. The training of the network on several samples of noisy data increases generalization capability and makes the network more robust.[15]

It is clear that the described procedure can be expanded to include a higher amount of noise by further augmenting the training and target matrices with noisy data. This method of training using augmented matrices is known as batch training in contrast to pattern training, where the inputs are given sequentially to the network. Utilizing a batching operation is often more efficient and provides a more accurate estimate of the gradient vector used in backpropagation.[13]

Damage Identification

Neural network B is used for damage identification. The input to the neural network is the matrix $\boldsymbol{P}$ corresponding to the damage (or damages) detected by network A. A separate network is used for each damage type. Once the type of damage is known, the problem is to determine the extent of damage. The target vector is defined in Eq. (10) for a single fault. For a compound fault, the target vector is a combination of the damage levels defined by Eq. (10). For example, for damage k, the neural network is trained for the following mapping:

$$\boldsymbol{d}_{\text{tr}} = \mathcal{N}(\boldsymbol{P}_k) \tag{23}$$

The issue of noisy data is also addressed for the damage identification network. This is done by defining the augmented matrix

$$\boldsymbol{P}_{k_n} = \lfloor \boldsymbol{P}_k \quad \boldsymbol{P}_k \quad \boldsymbol{P}'_k \quad \boldsymbol{P}''_k \rfloor \tag{24}$$

and the augmented target vector

$$\boldsymbol{d}_{\text{tr}_n} = \lfloor \boldsymbol{d}_{\text{tr}} \quad \boldsymbol{d}_{\text{tr}} \quad \boldsymbol{d}_{\text{tr}} \quad \boldsymbol{d}_{\text{tr}} \rfloor \tag{25}$$

where $\boldsymbol{P}'_k$ and $\boldsymbol{P}''_k$ are noisy signals generated using 5 and 10% noise contamination, respectively. The network mapping with noisy data is, therefore, given as

$$\boldsymbol{d}_{\text{tr}_n} = \mathcal{N}_n(\boldsymbol{P}_{k_n}) \tag{26}$$

Again, the ideal and noisy vectors have the same input targets. The network is first trained using ideal data [Eq. (23)], then trained using 10 cycles of noisy data [Eq. (26)], and finally trained with ideal data again.

Results and Discussion

For results, a four-bladed articulated rotor with properties similar to those of an SH-60 helicopter is selected (see Table 2). The rotor blade is modeled using 13 spatial finite elements along the bladespan. Six time finite elements with fourth-order shape functions are used along the azimuth to calculate the blade response. The results are obtained for a normalized rotor thrust coefficient $C_T/\sigma = 0.0726$ and a rotor advance ratio of $\mu = 0.3$. Selected validation of rotor component loads using this simulation for a baseline configuration are provided in Ref. 7. The results in this paper use relative changes in the rotor response and vibration predicted by the mathematical model for a faulty rotor to train the neural network. Furthermore, noise is added to the model predictions. These measures reduce the influence of modeling limitations and uncertainties on the fault detection results predicted by the trained neural network.

Faults Used for Damage Detection

Three faults are selected in this study to study the detection of compound faults using neural networks. These are damaged lag damper, damaged pitch-control system, and moisture absorption. Several combinations of faults on the damaged blade are also considered.

Table 2 Helicopter properties

Rotor radius	26.8 ft
Flap and lag hinge offset	15 in.
Number of blades	4
Blade chord	20.76 in.
Linear aerodynamic twist	−18 deg
C_l	6.0α
C_d	$0.002 + 0.2\alpha^2$
C_m	0
Lock number	8.00
Solidity	0.0826
Blade attachment point	41.5 in.
Rotor tip speed	725 ft/s
Helicopter weight	16,500 lb
Blade mass	235 lb

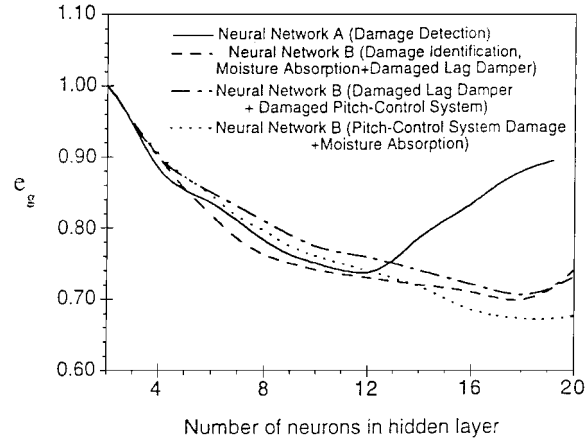

Fig. 4 Network error for generalization with increasing number of neurons in hidden layer, normalized by error of generalization with two neurons (all test data presented simultaneously to the trained network).

Number of Neurons

Training for both networks A and B is started using one neuron in the hidden layer. The number of neurons in the hidden layer is progressively increased from one, and the error for generalization of the network is monitored. The error for generalization is defined as

$$e_g = \frac{\| t_{\text{test}} - t_{\text{output}} \|}{\| t_{\text{test}} \|} \tag{27}$$

where t_{test} is the desired output and t_{output} is the estimated output of the trained network when presented with test data. The lower the value of e_g is, the better the network is at generalizing from training data.

Both ideal and noisy data are used for training and testing the network. All training data are presented to the network simultaneously for all damage levels defined by $\boldsymbol{d}_{\text{tr}}$. Once the network has trained, test data are presented to the trained network simultaneously for all damage levels defined by $\boldsymbol{d}_{\text{test}}$. Both primary and compound faults are considered. The error for generalization is shown in Fig. 4, as the number of neurons in the hidden layer is increased, for neural networks A and B (three combinations of damages). As the number of neurons increases from two, the error for generalization first decreases rapidly and reaches a minimum, after which it starts increasing slowly. For network A, e_g is minimum at 12 neurons and for network B at around 18 neurons (for three damage combinations). Therefore, networks A and B display good generalization characteristics with 12 and 18 neurons, respectively. Further results in this study use 12 neurons in the hidden layer for network A and 18 neurons for network B.

Damage Detection

Training and Testing

Network A is trained using simulated fault data for the three damages over the full range of damage level $\boldsymbol{d}_{\text{tr}}$ [Eq. (10)]. This includes individual as well as combinations of the damages. Training data for the three damages at damage levels $\boldsymbol{d}_{\text{tr}}$ are simultaneously presented to the neural network as matrix $\boldsymbol{P}_n$. Once the network is trained, the ability of the network to fit the training data exactly is verified. Then, the test data corresponding to damage levels $\boldsymbol{d}_{\text{test}}$ [Eq. (11)] are analyzed. Both ideal and noise contaminated test data are used. The test data are also simultaneously presented to the trained network for the three damages at damage levels defined by $\boldsymbol{d}_{\text{test}}$. For ideal test data, the network identifies the damage perfectly. Perfect identification implies that the target matrix $\boldsymbol{T}$ has the 1s and 0s in the correct places, as shown in Eq. (16).

The trained network is also used to identify damage from noise contaminated data. For noise contaminated test data, the network may make errors as noise levels are increased. As noise levels in the test data are increased, some of the elements of the target matrix are placed into the wrong position by the neural network. The number of errors made by network A is defined as the number of columns in target matrix $\boldsymbol{T}$ where the 1s and 0s are misplaced and is denoted by N_e. Figure 5 shows the number of errors made by the network

Table 3 Moderate and significant harmonics of system parameters (per revolution)

Δv	Δw	$\Delta\phi$	ΔF_x	ΔF_y	ΔF_z	ΔM_x	ΔM_y	ΔM_z
0	0	3	1	1	1	0	1	0
1	1	4	4	5	2	1	4	4
	3		5	6	3	2	6	5
			6	8	5	4	8	6
			9		8	6		10
			10		10			

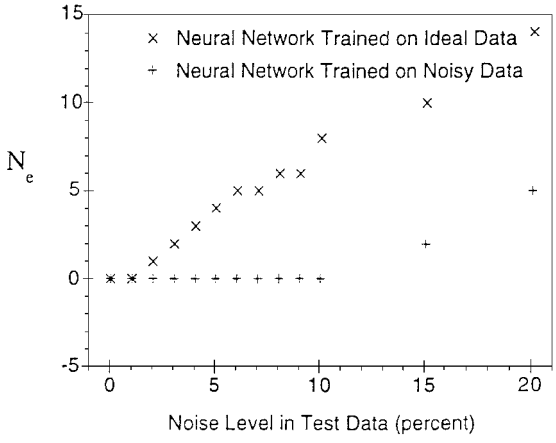

Fig. 5 Number of errors in pattern classification with increasing noise level for neural network trained on ideal data and noisy data (all test data presented simultaneously to the trained network).

with increasing noise levels in the test data. For comparison, results from a network trained on ideal data alone are also shown. For a network trained on ideal data alone, it is found that the network begins to misidentify damage even in the presence of low levels of noise (as low as 2%) in the test data. However, the network trained on noisy data produces no classification error for noise less than 10% and relatively small error at even higher noise levels, compared to the network trained on ideal data alone. This illustrates the benefits of training the neural network using noisy data. Note that the network is trained on noisy data corresponding to 5 and 10% noise contamination only, for 10 cycles.

Reduction in System Parameters Used for Training

The neural network uses all 159 rows of the training vector $\boldsymbol{p}$ corresponding to the first five harmonics of the lag, flap and torsion response, and the first 10 harmonics of the 3 hub forces and 3 hub moments. However, many of the elements in $\boldsymbol{p}$ are negligible, and it is likely that the neural network makes the pattern classification using only a subset of the system characteristics it receives. To reduce the size of the input vector, the rows of input matrix $\boldsymbol{P}$ and $\boldsymbol{P}_n$ for which all elements are negligible are deleted. The definition of negligible is given in Table 1. The remaining rows in the input matrix corresponding to system parameters that are moderate or significant, for at least one damage case, are shown in Table 3. By removing the negligible components of the input data, the number of rows in $\boldsymbol{P}$ is reduced from 159 to 70. After deleting the negligible system parameters, the network is again trained and tested using the reduced data. The network gives the same results after removal of the negligible inputs, compared to when all inputs are used. This reduced set of network input is used for subsequent results.

Minimum Higher Harmonic System Parameters

To determine the absolute minimum of inputs necessary, each input is eliminated one by one. Higher harmonic inputs are eliminated first. The final data set that is able to satisfy training and testing criteria consists of steady lag response, steady and 1/revolution flap and torsion response, 1/revolution and 4/revolution longitudinal and lateral force, 1/revolution and 3/revolution vertical force, 4/revolution rolling moment, 1/revolution pitching moment, and 1/revolution and 4/revolution yawing moments. These system parameters define the lowest harmonics of the system parameters that must be monitored to detect the three damages considered in this study (Table 4). The elements of Table 4 are a subset of the elements in Table 3 and can be used to lower the number of rows in the $\boldsymbol{P}$ matrix from 70 to 26. However, if more damage types are present than the three considered in this study, additional system parameters may have to be monitored.

Sequential Testing

The results just discussed were for cases when the neural network was simultaneously presented with test data for the three damages at 10 damage levels each. This procedure of batch, or parallel, testing is useful in determining the network generalization capability and in network sensitivity studies discussed earlier. However, in an actual helicopter, any damage will manifest itself by changes in system parameter vector $\boldsymbol{p}$ corresponding to any one damage at one damage level. The damage detection scheme must be able to detect damage from the input vector $\boldsymbol{p}$. To simulate this condition, the neural network trained using system parameters in Table 4 is sequentially presented with system response vector $\boldsymbol{p}$ for a given damage at a damage level selected from $\boldsymbol{d}_{\text{test}}$. The correct network output is then a vector $\boldsymbol{t}$, which is {1, 0, 0} for moisture absorption, {0, 1, 0} for lag damper damage, and {0, 0, 1} for the damaged pitch-control system. If the correct output is obtained when the network is presented with vector $\boldsymbol{p}$, the network has detected the damage. Figures 6–8

Table 4 Lowest harmonics of system parameters needed for detection (per revolution)

Δv	Δw	$\Delta\phi$	ΔF_x	ΔF_y	ΔF_z	ΔM_x	ΔM_y	ΔM_z
0	0	0	1	1	1	4	1	1
	1	1	4	4	3			4

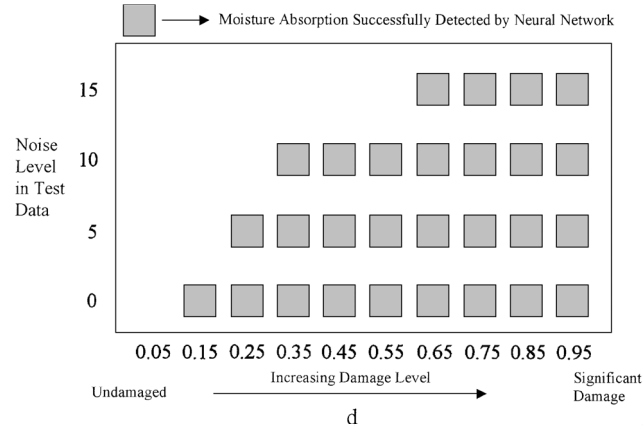

Fig. 6 Detection of moisture absorption by trained neural network when sequentially presented with rotor-system response test data at several damage levels.

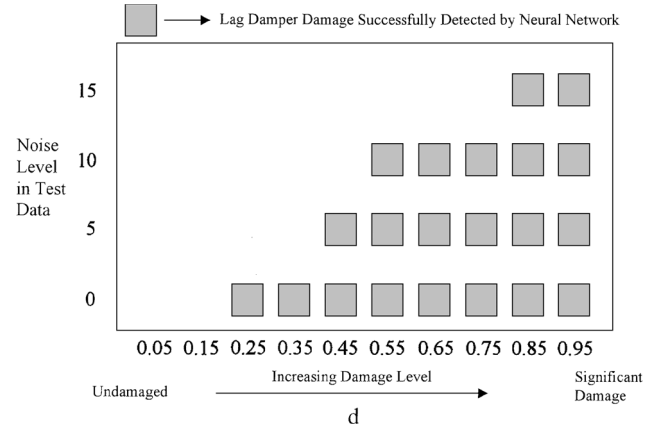

Fig. 7 Detection of damaged lag damper by trained neural network when sequentially presented with rotor-system response test data at several damage levels.

summarize the detection results for test data $\boldsymbol{p}$ at several noise levels and damage levels. The shaded squares in Figures 6–8 indicate successful detection of the damage by the neural network at a given noise level and damage level. The blank portions indicate a misdetection.

For ideal test data, moisture absorption can be detected for damage level $\boldsymbol{d} \geq 0.15$ and for damaged lag damper and damaged pitch-control system, for $\boldsymbol{d} \geq 0.25$. As the noise contamination of the test data increases, it becomes progressively difficult for the neural network to correctly detect faults at small damage levels. It appears from these figures that moisture absorption is easier to detect than the other damages and that faults with high damage levels ($\boldsymbol{d} \geq 0.85$) can be detected even when the system response data have significant noise contamination.

Next, combinations of the faults are investigated. To simulate this condition, the neural network is presented with the system response vector $\boldsymbol{p}$ for two damages at two damage levels. The correct network output is then {1, 1, 0} for moisture absorption and damaged lag damper, {1, 0, 1} for moisture absorption and damaged pitch-control system, and {0, 1, 1} for damaged lag damper and damaged pitch-control system. If the correct output is obtained when the network is presented with the vector $\boldsymbol{p}$, the network has detected the damage. Figure 9 shows the detection results at several noise levels and several damage levels for the compound fault consisting of moisture absorption and damaged lag damper. Results are shown for four cases with noise levels in the test data increasing from 0 to 15%. Successful fault detection by the neural network is represented by the shaded squares shown in the figure. The blank portions show misdetection. At low noise levels even small damage levels can be detected. However, as the noise level in the test data increases, it becomes difficult to detect damages at small damage levels. Similar results for moisture absorption and damaged pitch-control system are shown in Fig. 10 and for damaged lag damper and damaged pitch-control system are shown in Fig. 11.

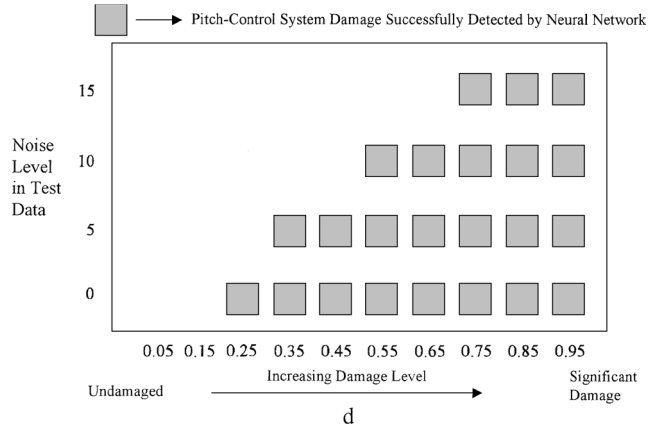

Fig. 8 Detection of damaged pitch-control system by trained neural network when sequentially presented with rotor-system response test data at several damage levels.

Damage Identification

Training and Testing

Once the damage has been detected, the next step is damage extent identification, i.e., to estimate the degree of damage. Neural network B is used for this damage identification. The reduced data set of system parameters shown in Table 4 is used for training and testing the network. The neural network is trained to map the training data to the rotor system parameters corresponding to the damage level $\boldsymbol{d}_{\text{tr}}$. Both ideal and noise contaminated training data are used.

Figure 12 shows the identification error varying with the noise level in the test data for moisture absorption. The identification error is defined as

$$e_{\text{id}} = \frac{\|\boldsymbol{d}_{\text{test}} - \boldsymbol{d}_{\text{output}}\|}{\|\boldsymbol{d}_{\text{test}}\|} \tag{28}$$

where $\boldsymbol{d}_{\text{test}}$ is the desired output of the trained network when exposed to test data and $\boldsymbol{d}_{\text{output}}$ is the actual output of the network. Other faults (both primary and compound) show similar results. For comparison,

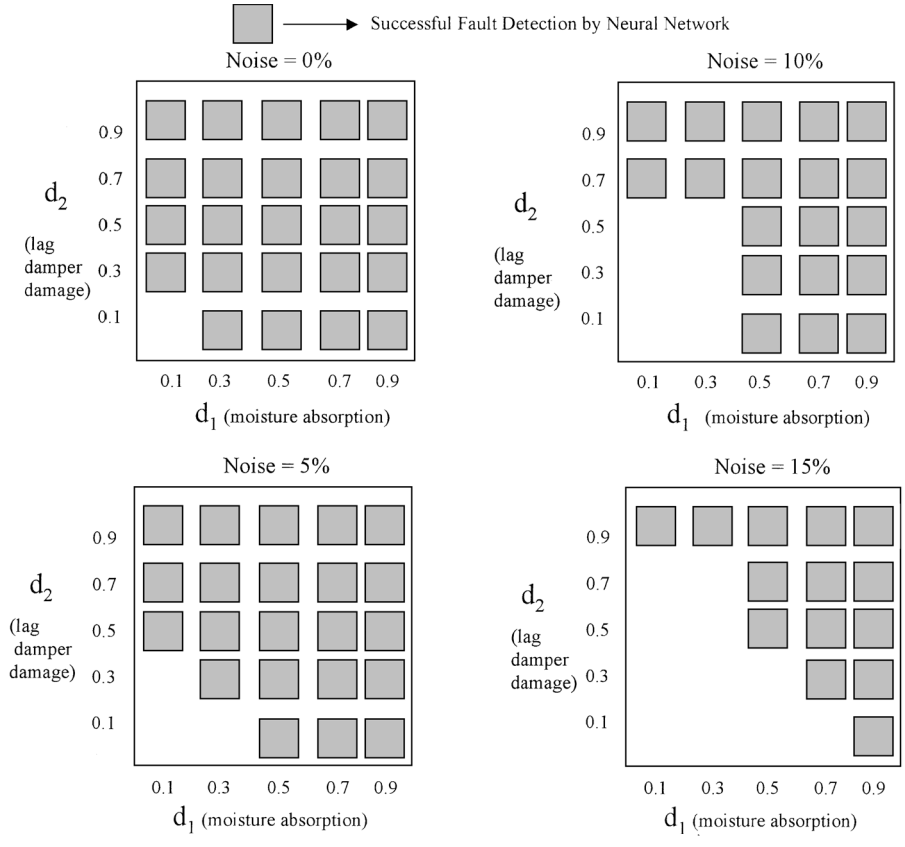

Fig. 9 Detection of moisture absorption and damaged lag damper compound fault by trained neural network when sequentially presented with rotor-system response test data at several damage levels and noise levels.

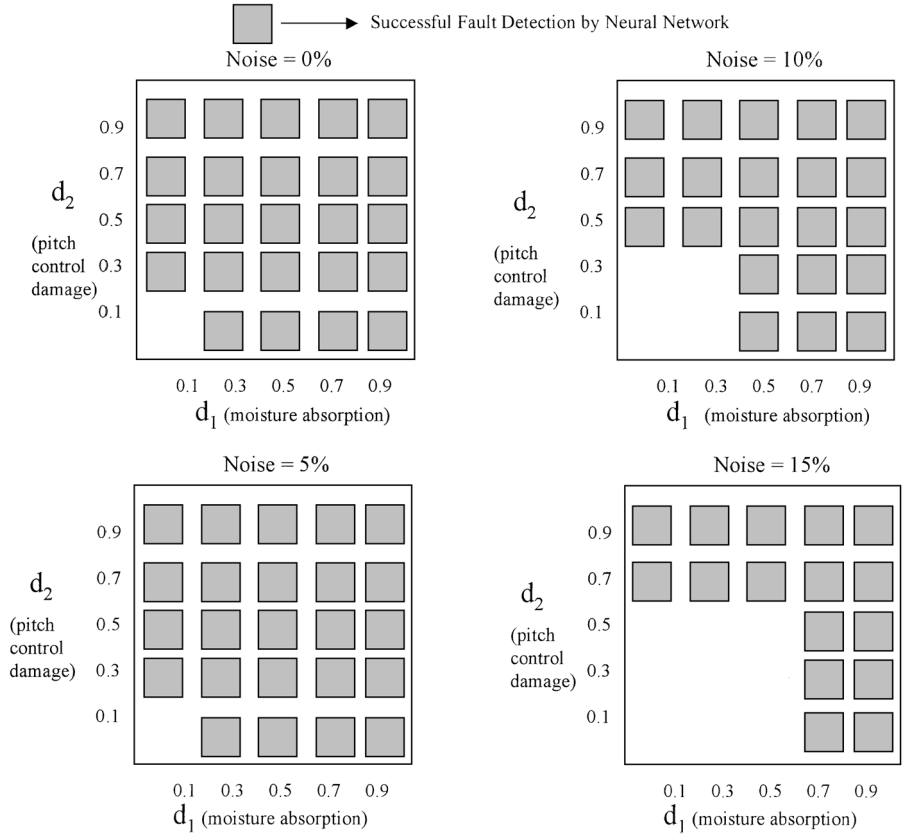

Fig. 10 Detection of moisture absorption and damaged pitch-control system compound fault by trained neural network when sequentially presented with rotor-system response test data at several damage levels and noise levels.

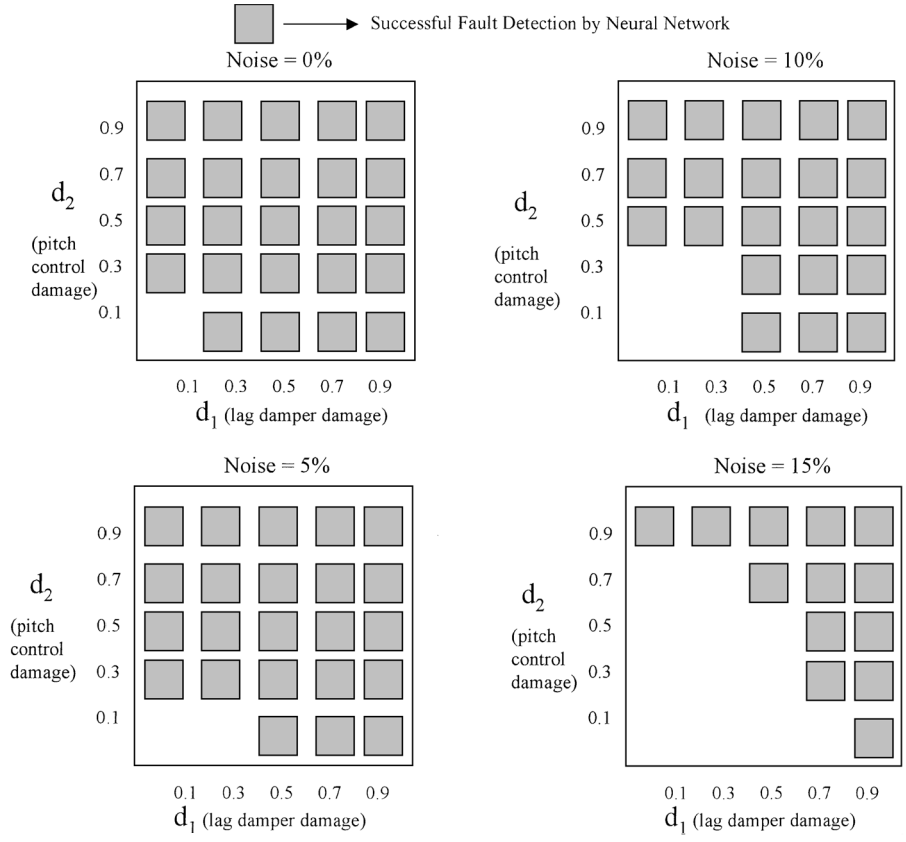

Fig. 11 Detection of damaged pitch-control system and damaged lag damper compound fault by trained neural network when sequentially presented with rotor-system response test data at several damage levels and noise levels.

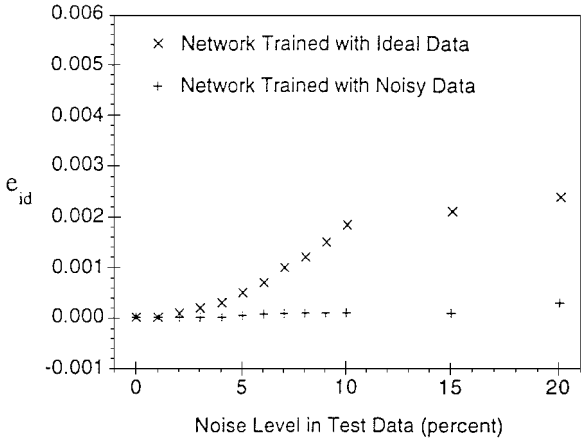

Fig. 12 Error in damage identification for moisture absorption with increasing noise level in test data.

the figure also shows the error of a network trained on ideal data alone. For a noise level below 2%, the network trained with ideal data shows zero error. However, as the noise level increases above 2%, the network trained on ideal data shows increasing error in identification. In contrast, the network trained on noisy data gives almost zero error for noise levels less than 10%, and low error even at noise levels of 15 and 20%. Note that the noisy training data include 5 and 10% noise contamination only, for 10 cycles.

Conclusions

Simulated fault data from the damaged rotor system are used to develop a neural network-based approach for rotor-system damage detection. Damages used for training the neural network include moisture absorption, damaged lag damper, and damaged pitch-control system. Both single faults and multiple faults are considered on the damaged blade. Relative changes in rotor blade response and vibration due to the presence of faults are used to train neural networks for damage detection and identification. The following conclusions are drawn from this study.

1) A feedforward neural network using backpropagation learning and one hidden layer can detect and quantify damage after being trained on simulated ideal and noise contaminated data obtained at several damage levels. Damage can be detected for both single faults and multiple faults on the damaged blade.

2) For accurate estimation of the type and extent of damages, it is important to train neural networks with noise contaminated response data. A neural network trained on ideal simulated data shows large errors when even a small amount of noise is presented in the test data.

3) For the faults considered in this study, a neural network with an input layer, a hidden layer, and an output layer is used. The number of neurons in the input and output layers is fixed by the size of the input and output data. For damage detection 12 neurons in the hidden layer are found to give a low error of generalization. For damage identification, 18 neurons in the hidden layer are found to give low error of generalization.

4) When the blade tip response, hub forces, and hub moments are used together to train the network, damage can be detected without relying significantly on higher harmonic data. For the damages investigated it was found that monitoring the steady lag, flap, and torsion response; 1/revolution flap and torsion response; 1/revolution and 4/revolution longitudinal and lateral forces; 1/revolution and 3/revolution vertical forces; 4/revolution rolling moment; 1/revolution pitching moment; and 1/revolution and 4/revolution yawing moment data was sufficient for detection and identification.

Acknowledgments

This work was sponsored by the U.S. Naval Surface Warfare Center, Carderock Division. The Project Monitor is Wayne Boblitt.

References

[1]Land, J., and Weitzman, C., "How HUMS Systems have the Potential for Significantly Reducing the Direct Operating Costs of Modern Helicopters Through Monitoring," American Helicopter Society 51st Annual Forum, Fort Worth, TX, May 1995.

[2]Chronkite, J. D., "Practical Application of Health and Usage Monitoring (HUMS) to Helicopter Rotor, Engine and Drive System," American Helicopter Society 49th Annual Forum, St. Louis, MO, May 1993.

[3]Carlson, R. G., Kershner, S. D., and Sewersky, R. A., "Sikorsky Health and Usage Monitoring System (HUMS) Program," American Helicopter Society 52nd Annual Forum, Washington, DC, June 1996.

[4]Cleveland, G. P., and Trammel, C., "An Integrated Health and Usage Monitoring System for the SH-60B Helicopter," American Helicopter Society 52nd Annual Forum, Washington, DC, June 1996.

[5]Azzam, H., and Andrew, M. J., "The Use of Math-Dynamic Models to Aid the Development of Integrated Health and Usage Monitoring Systems," *Journal of Aerospace Engineering*, Pt. G, Vol. 206, No. 1, 1992, pp. 71–96.

[6]Ganguli, R., Chopra, I., and Haas, D. J., "Formulation of a Helicopter Rotor-System Damage Detection Methodology," *Journal of the American Helicopter Society*, Vol. 41, No. 4, 1996, pp. 61–73.

[7]Ganguli, R., Chopra, I., and Haas, D. J., "Helicopter Rotor-System Damage Detection," Aeromechanics Meeting of the American Helicopter Society, Fairfield County, CT, Oct. 1995.

[8]Ganguli, R., Chopra, I., and Haas, D. J., "Detection of Simulated Helicopter Rotor System Faults Using Neural Networks," *Proceedings of the AIAA/ASME/ASCE/AHS/ASC 37th Structures, Structural Dynamics, and Materials Conference and Adaptive Structures Forum*, AIAA, Reston, VA, 1996.

[9]Schoess, J., Malver, F., Iyer, B., and Kooyman, J., "Rotor Acoustic Monitoring System (RAMS)—An Application of Acoustic Emission Integrity Monitoring and Assessment," American Helicopter Society 52nd Annual Forum, Washington, DC, June 1996.

[10]Haas, D. J., and Schaefer, C. G., Jr., "Emerging Technologies for Rotor System Health Monitoring," American Helicopter Society 52nd Annual Forum, Washington, DC, June 1996.

[11]Scully, M. P., "Computation of Helicopter Rotor Wake Geometry and its Influence on Rotor Harmonic Airloads," ASRL TR 178-1, Massachussetts Inst. of Technology, Cambridge, MA, March 1975.

[12]Leishman, J. G., and Beddoes, T. S., "A Generalized Model for Unsteady Aerodynamic Behavior and Dynamic Stall Using the Indicial Method," *Journal of the American Helicopter Society*, Vol. 36, No. 1, 1990, pp. 23–42.

[13]Haykin, S., *Neural Networks—A Comprehensive Foundation*, Macmillan, New York, 1994.

[14]Vogl, T. P., Mangis, J. K., Rigler, A. K., Zink, W. T., and Alkon, D. L., "Accelerating the Convergence of the Backpropagation Method," *Biological Cybernatics*, Vol. 59, No. 2, 1988, pp. 257–263.

[15]Holmstrom, L., and Koistinen, P., "Using Additive Noise in Back Propagation Training," *IEEE Transactions on Neural Networks*, Vol. 3, No. 1, 1992, pp. 24–38.

A. M. Waas
Associate Editor